

Review

Guanine Quadruplex Electrochemical Aptasensors

Ana-Maria Chiorcea-Paquim and Ana Maria Oliveira-Brett *

Department of Chemistry, Faculty of Science and Technology, University of Coimbra, 3004-535 Coimbra, Portugal; anachior@ipn.pt

* Correspondence: brett@ci.uc.pt; Tel.: +351-239-854-487

Academic Editors: Paolo Ugo and Ligia Moretto

Received: 9 May 2016; Accepted: 26 July 2016; Published: 30 July 2016

Abstract: Guanine-rich nucleic acids are able to self-assemble into G-quadruplex four-stranded secondary structures, which are found at the level of telomeric regions of chromosomes, oncogene promoter sequences and other biologically-relevant regions of the genome. Due to their extraordinary stiffness and biological role, G-quadruplexes become relevant in areas ranging from structural biology to medicinal chemistry, supra-molecular chemistry, nanotechnology and biosensor technology. In addition to classical methodologies, such as circular dichroism, nuclear magnetic resonance or crystallography, electrochemical methods have been successfully used for the rapid detection of the conformational changes from single-strand to G-quadruplex. This review presents recent advances on the G-quadruplex electrochemical characterization and on the design and applications of G-quadruplex electrochemical biosensors, with special emphasis on the G-quadruplex aptasensors and hemin/G-quadruplex peroxidase-mimicking DNAzyme biosensors.

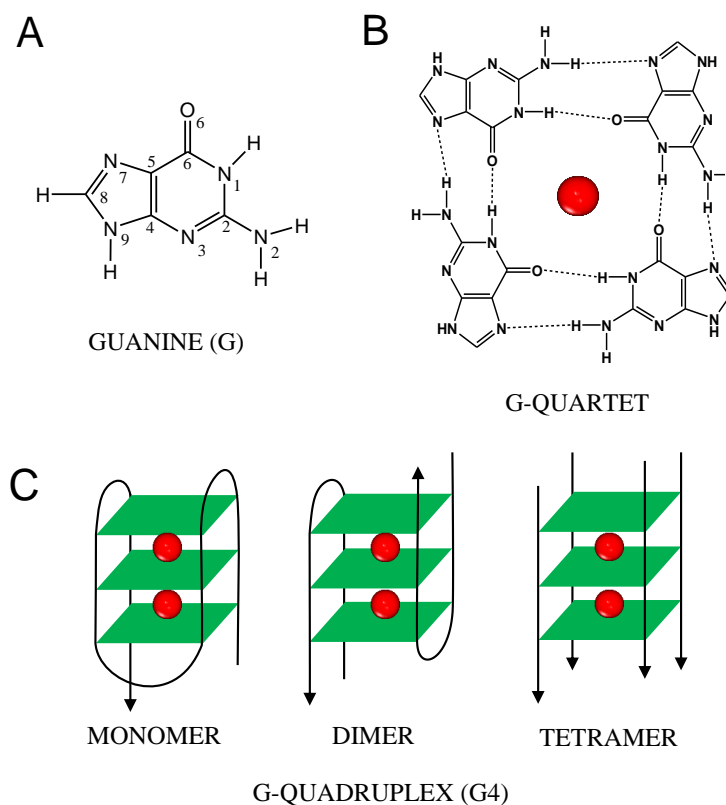
Keywords: G-quadruplex; G4; GQ; aptasensor; DNAzyme; DNA electrochemical biosensor

1. Introduction

DNA sequences rich in guanine (G) bases are able to self-assemble into four-stranded secondary structures called G-quadruplexes (G4 or GQ), (Scheme 1). The G4s are formed by G-quartet building blocks, which are planar associations of four G bases, held together by eight Hoogsteen hydrogen bonds (Scheme 1B). The G-quartets are stacked on top of each other, stabilized by π - π hydrophobic interactions and by monovalent cations, such as K^+ and Na^+ , which are coordinated to the lone pairs of electrons of O6 in each G.

The G4 structures are very polymorphic, being classified according to the number of strands (monomer, dimer or tetramer, Scheme 1C), according to strand polarity (i.e., the relative arrangement of adjacent strands in parallel or antiparallel orientations), glycosidic torsion angle (anti or syn) and the orientation of the connecting loops (lateral, diagonal or both) [1–4]. Different G4 topologies have been observed by nuclear magnetic resonance (NMR) or crystallography, either as native structures or complexed with small molecules [5].

The G4 sequences are found in chromosomes' telomeric regions, oncogene promoter sequences, RNA 5'-untranslated regions (5'-UTR) and other biologically-relevant regions of the genome, where they may influence the gene metabolism process and also participate in other important biological processes, e.g., DNA replication, transcriptional regulation and genome stability [1–14]. Moreover, G4 formation has been associated with a number of diseases, such as cancer, HIV and diabetes [3,5]. Due to their extraordinary stiffness and biological role, G4s become relevant in areas ranging from structural biology to medicinal chemistry, supra-molecular chemistry, nanotechnology and biosensor technology.



Scheme 1. (A) Chemical structure of the guanine (G) base; (B) G-quartet and (C) G-quadruplex (G4); the cations that stabilize the G4s are shown as red balls. Adapted from [14] with permission.

The G4 structures have emerged as a new class of cancer-specific molecular targets for anticancer drugs, since the G4 stabilization by small organic molecules can lead to telomerase inhibition and telomere dysfunction in cancer cells [2,15,16]. The G-rich oligonucleotides (ODNs) are also able to self-organize in G4-based two-dimensional networks and long nanowires, relevant for nanotechnology applications [17,18]; therefore, the assembly of G4 nanostructures and devices has been extensively revised in the literature [2,3,5,6,19].

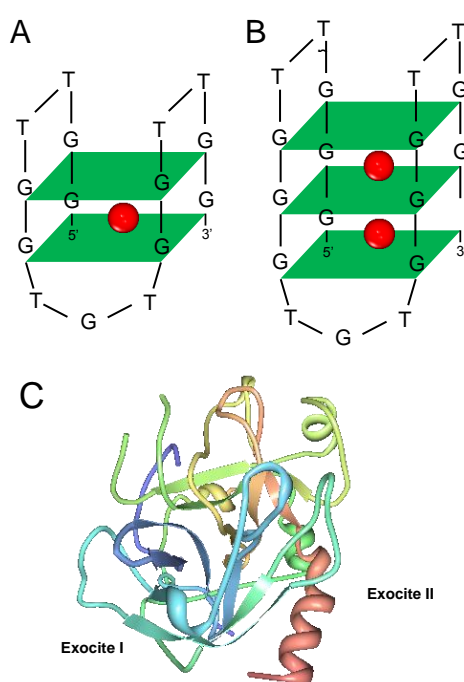
The G4 structures were studied using different experimental techniques, such as molecular absorption, circular dichroism, molecular fluorescence, mass spectrometry, NMR, surface plasmon resonance, crystallography or atomic force microscopy (AFM) [20–23]. The electrochemical research on DNA is of great relevance to explain many biological mechanisms, and the nucleic acids redox behavior and adsorption processes have been studied for a long time [24–31], but only recently started to be used for the detection of G4 configurations [19,31,32].

Aptamers are a special class of small synthetic oligonucleotides able to form secondary and tertiary structures, larger than small molecule drugs, but smaller than antibodies, with the advantage of being highly specific in binding to small molecules, proteins, nucleic acids and even cells and tissues [33–36]. The aptamers bind to the targets by a lock and key mode, and the name “aptamer” is from the Latin word *aptus*, meaning “to fit” [36]. Among them, short aptamers that adopt G4 configurations received increased attention, and the electrochemical sensing devices based on G4 nucleic acid aptamers are highly selective and sensitive, fast, accurate, compact, portable and inexpensive.

In this review, recent advances on the G4 structure in nucleic acid electrochemistry and the design and applications of the G4 electrochemical biosensors that use redox labels as amplification strategies, i.e., the G4 electrochemical aptasensors and the hemin/G4 HRP-mimicking DNAzyme electrochemical biosensors, will be presented.

2. G4 Electrochemistry

The first report on the electrochemical oxidation of G4 structures concerned the investigation of two, thrombin-binding aptamer (TBA) sequences, 15-mer $d(G_2T_2G_2TGTG_2T_2G_2)$ (Scheme 2A) and 19-mer $d(G_3T_2G_3TGT_3T_2G_3)$ (Scheme 2B), using differential pulse (DP) voltammetry at a glassy carbon electrode (GCE) [32,37]. The different adsorption patterns of the TBA sequences observed by AFM onto highly oriented pyrolytic graphite (HOPG) were correlated with their voltammetric behavior in the presence/absence of K^+ ions. In Na^+ -containing solutions, the oxidation of both TBA sequences showed one anodic peak corresponding to the oxidation of G residues in the TBA single strands. The G oxidation occurred at the C_8-H position, in a two-step mechanism involving the total loss of four electrons and four protons. Upon the addition of K^+ , both sequences folded into G4 structures, causing the decrease of the G oxidation peak current and the occurrence of a new G4 peak at a higher potential, due to the oxidation of G residues in the G4 configuration. In the absence of K^+ ions, in only Na^+ ion-containing solutions, G4 formation also occurred, but was much slower.



Scheme 2. Unimolecular antiparallel G4 structures formed by the thrombin binding aptamers (TBA): (A) $d(G_2T_2G_2TGTG_2T_2G_2)$ and (B) $d(G_3T_2G_3TGT_3T_2G_3)$; (C) thrombin tertiary structure. Adapted from [38] with permission.

The decrease of the G oxidation peak current was due to a decrease in the number of free G residues in single-stranded TBA, and the increase of the G4 oxidation peak current was due to an increased number of G4 structures that were more difficult to oxidize. The adsorption of TBA in a G4 conformation, as rod-like-shaped aggregates, was observed by AFM [32,37].

The 10-mer ODNs that contain blocks of 8–10 G residues, $d(G)_{10}$, $d(TG_9)$ and $d(TG_8T)$, form parallel tetra-molecular G4s (Scheme 1C, right) and were investigated by AFM and DP voltammetry. The influence of the ODN sequence and concentration, pH (Figure 1), the presence of monovalent cations, Na^+ vs. K^+ (Figure 2A,C), and incubation time (Figure 2B,C) was determined [19,32,39,40]. The formation of G4 structures and higher-order nanostructures, due to the presence of a long contiguous G region, and the influence of the thymine residues at the 5' and 3' molecular ends in $d(TG_9)$ and $d(TG_8T)$ were clarified. DP voltammetry allowed the detection of the single strands' association into G4s and G-based nanostructures, in freshly-prepared solutions, at concentrations 10-times lower than usually detected using other techniques currently employed to study the formation of G4s.

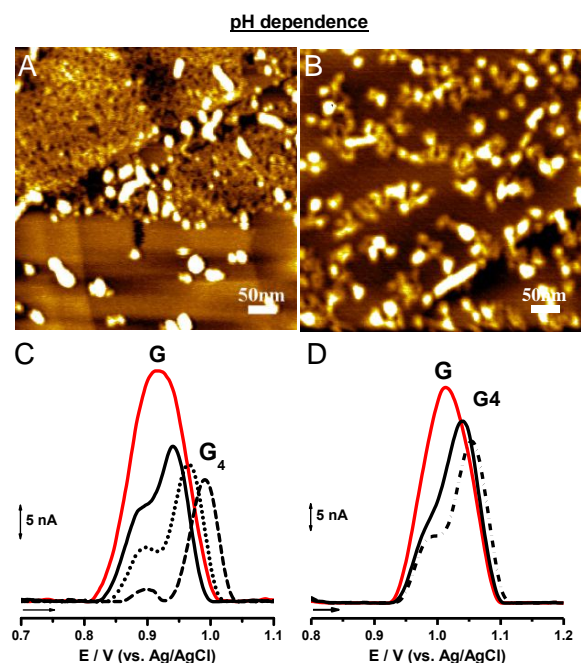


Figure 1. d(G)₁₀ sequence G4 formation pH dependence at (A,C) pH = 7.0 and (B,D) pH = 4.5: (A,B) AFM images of 0.3 μM d(G)₁₀ spontaneously adsorbed onto HOPG; and (C,D) bioelectrocatalyzed voltammograms baseline corrected of 3.0 μM d(G)₁₀ after (—) 0 h, (—) 24 h, (●●●) 72 h, (●●●) 5 days and (E, ■■■) 14 days of incubation. Adapted from [39] with permission.

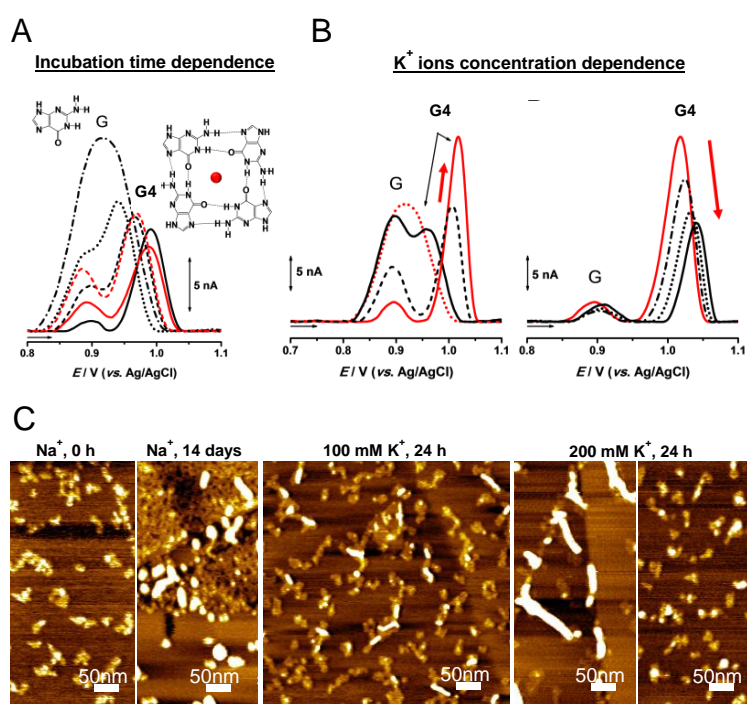


Figure 2. Incubation time and K⁺ ion concentration dependence on the G4 formation of the d(G)₁₀ sequence; (A,B) DP voltammograms baseline corrected for d(G)₁₀: (A) in the absence of K⁺ ions at (●●●) 0 h, (●●●) 24 h, (■■■) 48 h and (—) 14 days of incubation and in the presence of 1 mM K⁺ ions at (■■■) 0 h and (—) 24 h of incubation; (B) in the absence (●●●) and in the presence of (—, left) 100 μM, (■■■) 5 mM, (—) 100 mM, (●●●) 200 mM, (●●●) 500 mM and (—, right) 1 M K⁺ ions, 0 h of incubation; (C) AFM images of d(G)₁₀ in the absence/presence of different K⁺ ion concentrations and different incubation times. Adapted from [40] with permission.

Single-stranded ODNs were observed only in Na^+ ion solutions at short incubation times and were detected in AFM as thin polymeric structures and in DP voltammetry by the occurrence of only the G oxidation peak. The G4 structures were formed very slowly in Na^+ ions, after a long incubation time, faster in K^+ ions, after a short incubation time, and were detected by AFM as spherical aggregates and by DP voltammetry by the decrease of the G oxidation peak current and the occurrence/increase of the G4 oxidation peak current, as well as a shift to positive potentials, in a K^+ ion concentration- and in a time-dependent manner. The presence of K^+ ions strongly stabilizes and accelerates the G4 formation. For increased $\text{d}(\text{G})_{10}$ concentrations, long G-nanowires were formed, demonstrating the potential of G-rich DNA sequences as a scaffold for nanotechnological applications [19,32,39,40].

The *Tetrahymena* telomeric repeat sequence $\text{d}(\text{TG}_4\text{T})$ forms parallel-stranded tetra-molecular G4s in the presence of Na^+ and K^+ ions and is considered to be a simple model for biologically-relevant G4s. It has also provided high resolution structural data on drug-DNA interactions. The transformation of the $\text{d}(\text{TG}_4\text{T})$ from single-stranded into G4 configurations, influenced by the Na^+ and K^+ ion concentration, was successfully detected using AFM on HOPG and DP voltammetry at GCE (Figures 3 and 4) [41]. The $\text{d}(\text{TG}_4\text{T})$ in a G4 conformation self-assembled very quickly in K^+ ion solutions and slowly in Na^+ ion solutions. The optimum K^+ ion concentration for the G4 structure formation of $\text{d}(\text{TG}_4\text{T})$ was similar to the intracellular K^+ ion concentration of healthy cells. In the presence of Na^+ ions, $\text{d}(\text{TG}_4\text{T})$ also formed short nanowires and nanostructured films that were never observed in K^+ ion-containing solution, suggesting that the rapid formation of stable G4s in the presence of K^+ is relevant for the good function of cells.

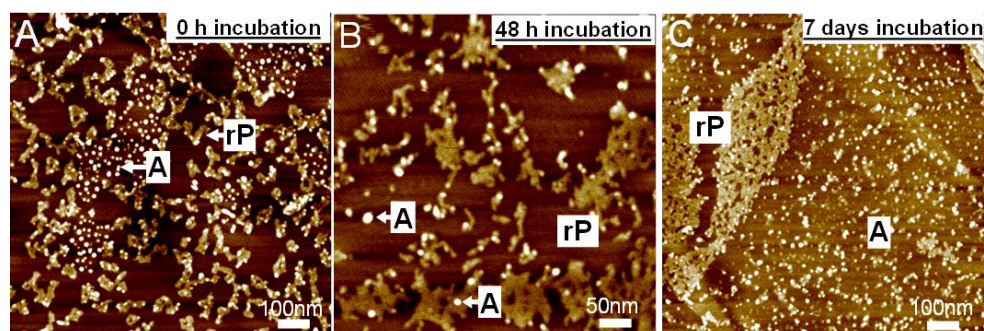


Figure 3. AFM images of $\text{d}(\text{TG}_4\text{T})$ in the presence of K^+ ions, after (A) 0 h; (B) 48 h and (C) 7 days of incubation. Adapted from [41] with permission.

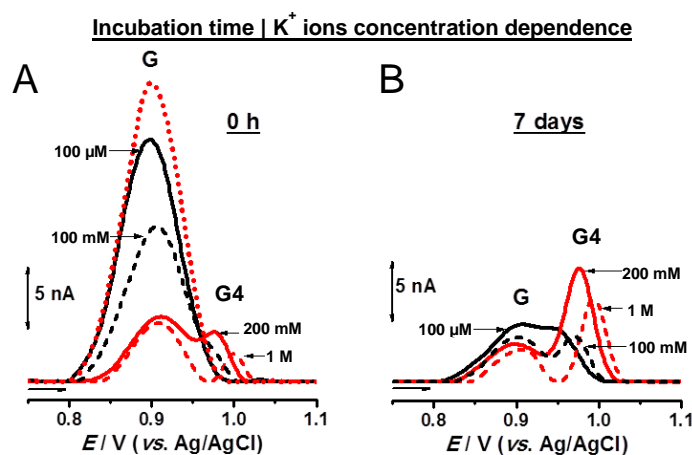


Figure 4. Incubation time and K^+ ion concentration dependence on the G4 formation of $\text{d}(\text{TG}_4\text{T})$. DP voltammograms baseline corrected for $\text{d}(\text{TG}_4\text{T})$, after (A) 0 h and (B) seven days of incubation; (A, $\bullet\bullet\bullet$) in the absence of K^+ ions and (A,B) in the presence of (—) 100 μM , ($\blacksquare\blacksquare\blacksquare$) 100 mM, (—) 200 mM and ($\bullet\bullet\bullet$) 1 M K^+ ions. Adapted from [41] with permission.

Synthetic polynucleotides poly(dG) and poly(G) are widely used as models to determine the interaction of drugs with G-rich segments of DNA. AFM and DP voltammetry showed that, at low incubation times, short G4 regions were formed along the poly(G) single-strands, while low adsorption large poly(G) aggregates in a G4 conformation were formed after high incubation times in the presence of either Na^+ or K^+ monovalent ions (Figure 5) [42]. The DP voltammetry in freshly-prepared poly(G) solutions showed only the G oxidation peak, due to the oxidation of G residues in the poly(G) single strand. Increasing the incubation time, the G oxidation peak current decreased; the peak disappeared; and the G4 oxidation peak in the poly(G) in a G4 conformation appeared, at a higher oxidation potential, depending on the incubation time, presenting a maximum after 10 days of incubation and reaching a steady current after ~ 17 days of incubation.

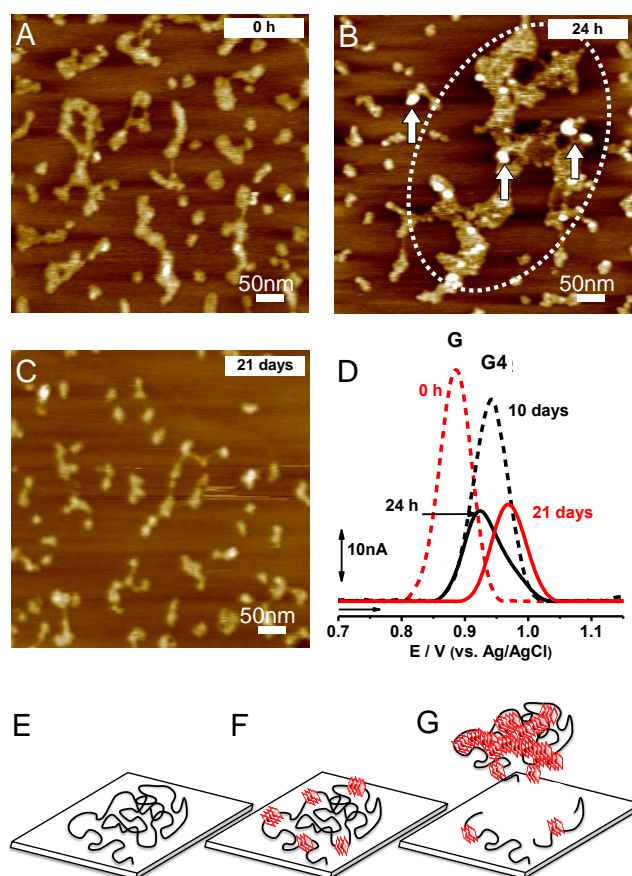


Figure 5. Poly(G) in the presence of K^+ ions: (A–C) AFM images, after: (A) 0 h, (B) 24 h and (C) 21 days of incubation; (D) DP voltammograms baseline corrected, after: (---) 0 h, (—) 24 h, (---) 10 days and (—) 21 days of incubation; (E–G) Schematic representation of the poly(G) adsorption process: (E) poly(G) single strand, (F) poly(G) single strand with short G4 regions and (G) poly(G) single strand with larger G4 regions. Adapted from [42] with permission.

The interaction between the TBA sequences $\text{d}(\text{G}_2\text{T}_2\text{G}_2\text{TGTG}_2\text{T}_2\text{G}_2)$ and $\text{d}(\text{G}_3\text{T}_2\text{G}_3\text{TGT}_3\text{T}_2\text{G}_3)$ and the serine protease thrombin (Scheme 2) was determined successfully by AFM and voltammetry, taking into account the thrombin interaction with TBA primary and secondary structures, as well as the thrombin folding in the presence of alkaline metals [32,38]. In the interaction, the TBA single strands coiled around thrombin, leading to the formation of a robust TBA-thrombin complex that maintained the thrombin symmetry and conformation, which resulted in the thrombin oxidation peaks, within the TBA-thrombin complex, occurring at more positive potentials, than in free thrombin. In the presence of K^+ , the TBA sequences were folded into a G4 conformation, which facilitated the interaction with thrombin. The TBA-thrombin complexes adsorbed on the carbon electrode with the TBA in contact with the surface and the thrombin on top, far from the surface; thus, the thrombin

molecule was less accessible to oxidation, also leading to the occurrence of the thrombin oxidation peaks at more positive potentials.

A large number of potent G4-binding ligands, which stabilize or promote G4 formation, has been described. Especially at the chromosomes' telomeric regions, the telomeric DNA is able to form G4 structures; therefore, the G4 ligands prevent the G4s from unwinding and opening the telomeric ends to telomerase, thus indirectly targeting the telomerase and inhibiting its catalytic activity.

A number of acridine derivatives have been specifically synthesized with the purpose of increasing binding affinity and selectivity for human telomeric G4 sequences found in chromosomes' telomeric regions, e.g., BRACO-19 [43] and RHPS4. More recently, a new series of triazole-linked acridine ligands, e.g., GL15 and GL7 [44], with enhanced selectivity for human telomeric G4s binding versus duplex DNA binding, have been designed, synthesized and evaluated.

The interactions of the GL15 triazole-acridine conjugate with the short-length *Tetrahymena* telomeric DNA repeat sequence d(TG₄T) and with the long chain poly(G) sequence, at the single-molecule level, by AFM and DP voltammetry, were investigated [45]. GL15 interacted with both the d(TG₄T) and poly(G) sequences, in a time-dependent manner, and the influence of Na⁺ vs. K⁺ ions was evaluated.

The G4 formation was detected in AFM, by the adsorption of small d(TG₄T) and poly(G) spherical aggregates, as well as large G4-based poly(G) assemblies, and the DP voltammetry showed the decrease and disappearance of the GL15 and the G oxidation peak currents and the appearance of the G4 oxidation peak (Figure 6). The GL15 strongly stabilized and accelerated the G4 formation in both Na⁺ and K⁺ ion-containing solutions, although only K⁺ promoted the formation of perfectly-aligned tetra-molecular G4s. The GL15-d(TG₄T) complex with the G4 configuration was discrete and approximately globular, whereas the GL15-poly(G) complex with the G4 configuration was formed at a number of points along the length of the polynucleotide, analogous to beads on a string.

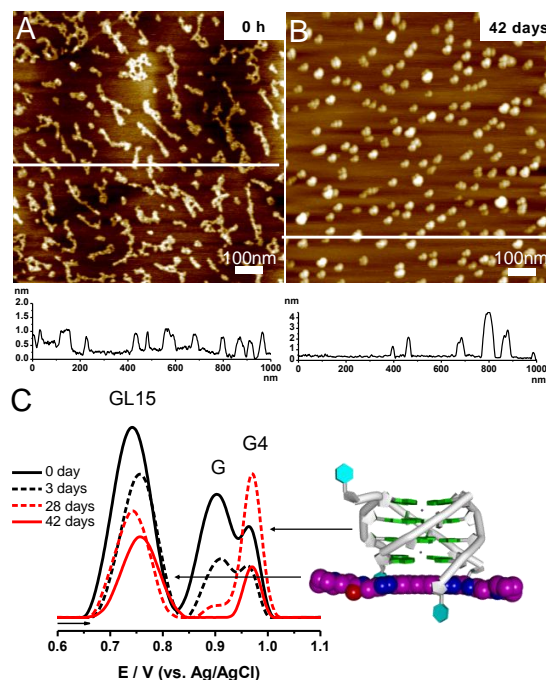


Figure 6. GL15-d(TG₄T) after different incubation times in the presence of K⁺ ions: (A,B) AFM images and cross-section profiles through the white dotted lines and (C) DP voltammograms baseline corrected. Adapted from [45] with permission.

3. G4 Electrochemical Biosensors

A DNA-electrochemical biosensor is formed by an electrode (the electrochemical transducer) with a DNA probe immobilized on its surface (the biological recognition element) and is used to detect

DNA-binding molecules (the analyte) that interact and induce changes in the DNA structure and electrochemical properties, which are further translated into an electrical signal [25–27,29–31,46,47]. Up to now, the G4-based electrochemical biosensors reported in the literature always used redox labels as amplification strategies. Two important types of G4 electrochemical biosensors, the G4 electrochemical aptasensors and the hemin/G4 DNAzyme electrochemical biosensors, will be revisited.

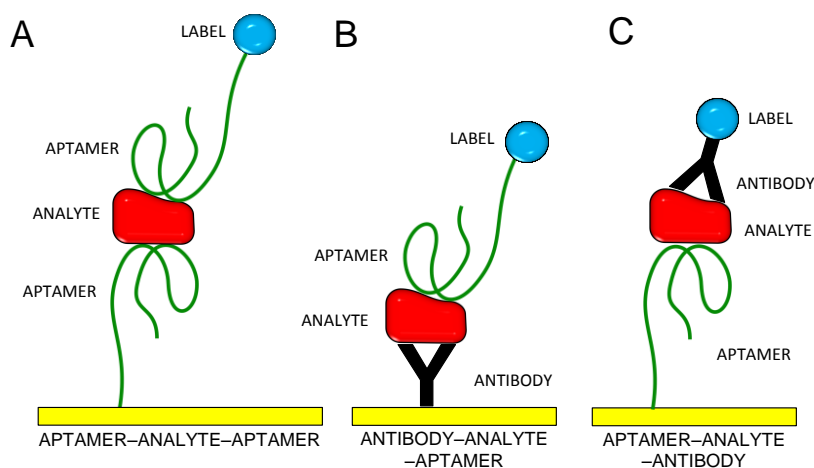
3.1. G4 Electrochemical Aptasensors

Aptamers are DNA or RNA sequences selected in vitro that present the ability to specifically bind a molecular target. Short aptamers that adopt G4 configurations can bind to a wide variety of molecular targets, mainly proteins (such as thrombin, nucleolin, signal transducer and activator of transcription STAT3, human RNase H1, protein tyrosine phosphatase Shp2, VEGF, HIV-1 integrase, HIV-1 reverse transcriptase, HIV-1 reverse transcriptase, HIV-1 nucleocapsid protein, *M. tuberculosis* polyphosphate kinase 2, sclerostin, insulin, etc.), but also some other targets (hematoporphyrin IX, hemin, ochratoxin, potassium ions, ATP) [33–35,48,49]. Many aptamers recognize specifically different positions on the analyte; for example, TBA recognizes the fibrinogen and heparin binding sites of thrombin.

The first G4 electrochemical aptasensors used TBA sequences and gold electrodes as electrochemical transducers, the aptamers' attachment being achieved using an amine or a thiol functionalization [50–52], or the affinity of biotin to avidin, streptavidin or neutravidin [53]. Depending on the assay format, two main G4 electrochemical aptasensor categories can be depicted, the sandwich-type aptasensors (also named dual-site binding) and the structure switching-based aptasensors (single-site binding) [54,55].

3.1.1. Sandwich-Type G4 Electrochemical Aptasensor

The aptamer–analyte–aptamer sandwich-type G4 electrochemical aptasensor (Scheme 3A) is composed by two aptamer layers, the first aptamer layer being immobilized on the electrode and used for capturing the analyte and the second aptamer layer being labelled and used for the electrochemical detection. The first aptamer was generally immobilized onto gold via a thiol [56–60] and, more recently, magnetic beads [61,62]. The labels of the second aptamer were either redox molecules, nanocomposites [60], nanoparticles [57,63], quantum dots [58,59] or enzymes, with catalytic activity that transformed the substrate into an electroactive product [56,64,65].



Scheme 3. Sandwich-type G4 electrochemical aptasensors: (A) aptamer–analyte–aptamer sandwich; the first aptamer is used for binding the analyte to the electrode, and the second labelled aptamer is used for detection; (B) antibody–analyte–aptamer sandwich; the analyte is bound to the surface via an antibody, and a labelled aptamer is used for detection; (C) aptamer–analyte–antibody sandwich; the analyte is bound to the surface via an aptamer, and a labelled antibody is used for detection. Adapted from [19] with permission.

The first G4 electrochemical aptasensor reported presented an aptamer–analyte–aptamer sandwich-type format, being developed for thrombin detection [64,65]. The sensor was built up by two aptamers, the first aptamer immobilized onto the gold electrode for capturing the thrombin onto it and the second one, a glucose dehydrogenase (GDH)-labelled anti-thrombin aptamer. The current increase generated by the electroactive product of the enzyme reaction was observed, and >10 nM thrombin were detected selectively. This approach proved for the first time that aptamers can be successfully employed in sandwich-type sensing devices, instead of and with advantages over antibodies.

Employing platinum nanoparticle labels as catalysts for the reduction of H₂O₂ to a TBA/thrombin complex allowed the amplified electrocatalytic detection of thrombin with a 1 nM detection limit [57].

In another report, gold nanoparticles' functionalization of the second aptamer improved the thrombin detection sensitivity, showing a 0.02 nM detection limit, with a 0.05–18 nM linear range [63].

The use of cadmium sulfide quantum dot labels of the secondary aptamer allowed thrombin detection with a 0.14 nM detection limit, corresponding to 28 fmol of analyte [58], while in another similar approach, thrombin determination in human serum showed a detection limit as low as 1 pM [59].

Using a more complex design, based on conductive graphene-3,4,9,10-perylenetetracarboxylic dianhydride nanocomposites as a sensor platform and PtCo nanochains–thionine–Pt–horseradish peroxidase-labelled secondary TBA for signal amplification, thrombin was detected at a linear range from 10⁻¹⁵–10⁻⁹ M and a 6.5 × 10⁻¹⁶ M detection limit [60].

In another approach, an aptamer–analyte–aptamer sandwich-type G4 electrochemical aptasensor was based on enzymatic labelling of the second aptamer with glucose dehydrogenase (GDH), measuring the electric current generated by the glucose oxidation catalyzed by GDH and selectively detecting 1 μM of thrombin [64].

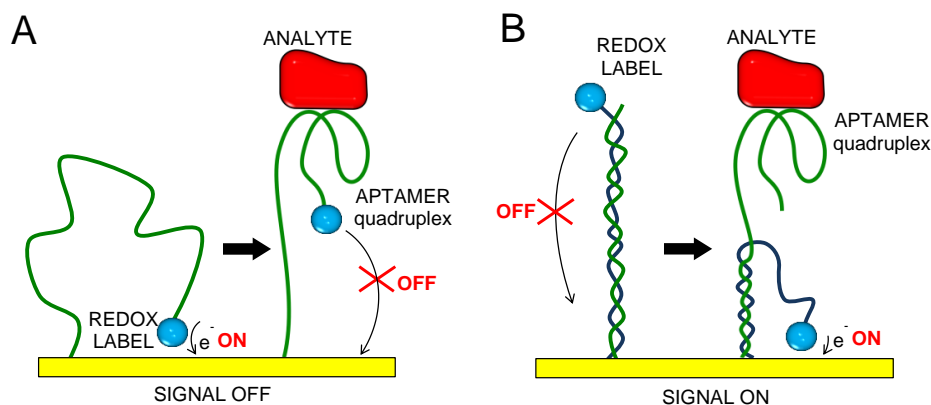
Apart from the aptamer–analyte–aptamer sandwich-type G4 electrochemical aptasensor, other design strategies were also employed. The antibody–analyte–aptamer sandwich-type aptasensor consisted of attaching the analyte to the surface via an antibody combined with a labelled aptamer that adopt the G4 configuration for detection (Scheme 3B). This sensor design was used to detect thrombin at a nanogold-chitosan composite-modified GCE, linked with the aptamer via a polyclone antibody. The electrochemical active marker used was methylene blue (MB) directly intercalated in the probing aptamer. The sensor linear response for thrombin was in the range 1–60 nM with a 0.5 nM detection limit [66].

The aptamer–analyte–antibody sandwich-type aptasensor consisted of attaching the analyte to the surface via an aptamer able to form the G4 structure, the detection being performed with a redox-labelled antibody (Scheme 3C) [67].

A sandwiched immunoassay for thrombin used a NH₂-functionalized-TBA immobilized on gold nanoparticle-doped conducting polymer nanorod electrodes and a ferrocene label bound to an antithrombin antibody [67]. The sensor used the electrocatalytic oxidation of ascorbic acid by the ferrocene moiety, presenting a wide dynamic range of 5–2000 ng·L⁻¹ and a low detection limit of 5 ng·L⁻¹ (0.14 pM) and was tested in a real human serum sample for the detection of spiked concentrations of thrombin.

3.1.2. Structure-Switching G4 Electrochemical Aptasensor

A different category of G4 electrochemical aptasensors is based on the aptamer structural modifications upon binding the analyte from the single-stranded to the G4 configuration, structure-switching G4 electrochemical aptasensor (Scheme 4). This strategy generally involved the direct immobilization of the aptamer on the electrode surface, while the analyte was present in solution. The electrochemical signal amplification was obtained by labelling the aptamer with a redox tag [68,69].



Scheme 4. Structure-switching G4 electrochemical aptasensors: the aptamer is modifying its conformation after analyte binding: (A) increasing the distance from the redox label to the electrode (signal off); (B) decreasing the distance from the redox label to the electrode (signal on). Adapted from [19] with permission.

The majority of structure-switching G4 electrochemical aptasensors were developed using gold electrodes, although, more recently, other electrochemical transducers have been employed, such as gold disk microelectrode arrays [70], modified platinum [71] or carbon electrodes [63,71–75].

The first report on a structure-switching G4 electrochemical aptasensor used a covalently-attached MB-labelled TBA on a gold electrode [68,76]. The aptasensor detection type was signal-off (Scheme 4A), i.e., in the absence of the thrombin target, the immobilized TBA remained relatively unfolded, allowing the electron transfer from the MB label to the electrode surface, while after thrombin binding, the formation of TBA in the G4 configuration was induced, which inhibited the electron transfer (Figure 7A).

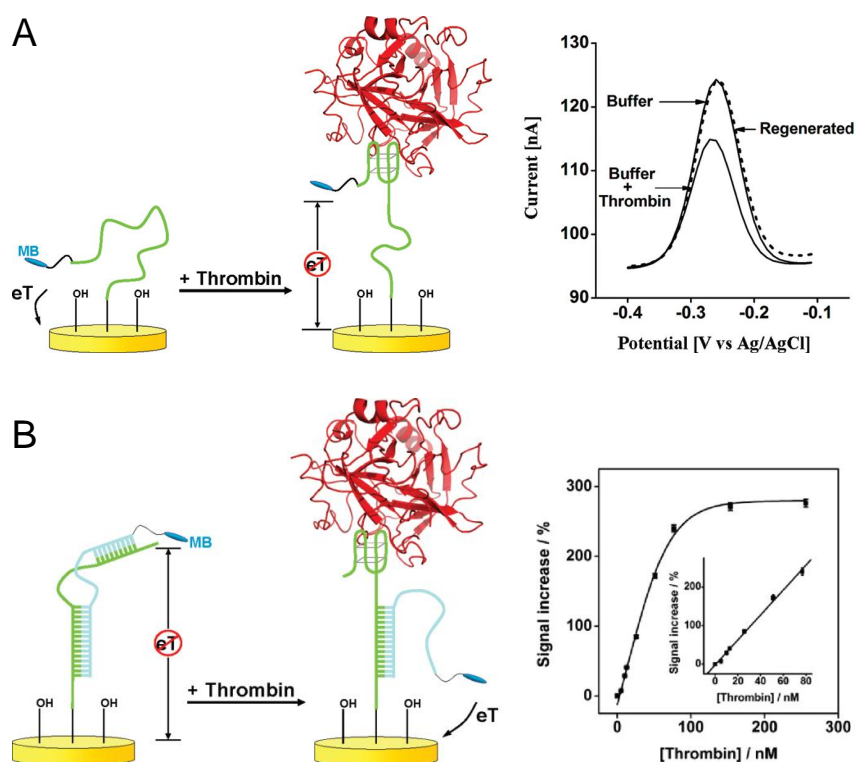


Figure 7. Structure-switching G4 electrochemical aptasensor for thrombin: (A) signal off: thrombin binding reduces the current from the MB redox tag; and (B) signal on: thrombin binding increases the current from the MB redox tag. Reproduced from [68] with permission.

The sensor was selective enough to detect thrombin directly in blood serum with a 20 nM thrombin detection limit. Similar G4 electrochemical aptasensors for thrombin were developed in parallel, using ferrocene labels [77–79]. In another design, a beacon aptamer-based biosensor for thrombin showed a linear signal between 0 and 50.8 nM of thrombin, with a 0.999 correlation factor and an 11 nM detection limit [80].

A bifunctional aptamer-based electrochemical biosensor for the detection of both thrombin and adenosine was developed [81]. The TBA was first immobilized on a gold electrode, and then, it was hybridized with an adenosine aptamer and labelled with MB. In the presence of thrombin or adenosine, the aptamer bonded to thrombin or to adenosine instead of MB, and the decrease of the MB peak current was related to the concentration of either thrombin or adenosine. The sensor showed a 3 nM thrombin and a 10 nM adenosine detection limit.

A signal-on structure-switching G4 electrochemical aptasensor (Scheme 4B) was described [82], with a short MB-tagged oligonucleotide hybridized with both the thrombin-binding portion of the TBA and the DNA sequence linking the aptamer to the electrode. The thrombin binding induced the structural modification of the TBA in a G4 configuration, liberating the 5' end of the tagged oligonucleotide to produce a flexible, single-stranded sequence, which allowed the MB tag to react at the electrode surface, increasing the reduction peak current (Figure 7B). Comparing to the signal-off structure-switching G4 electrochemical aptasensors previously described [68,76], the signal-on aptasensor design achieved a current increase of ~ 300% with a saturated target and a 3 nM detection limit [82].

Apart from MB, other redox labels have also been employed. Among them, ferrocene [72,83–89] and $\text{Ru}(\text{NH}_3)_6^{3+}$ [75,90] were very popular, especially for the construction of impedimetric aptasensors.

An impedimetric aptasensor for thrombin detection was described, based on different TBA sequences directly immobilized on the gold electrode and using phosphoramidite synthons for a strong thiolate anchoring of the aptamer and high flexibility [83]. In the presence of the $[\text{Fe}(\text{CN})_6]^{3-/4-}$ redox probe, the impedimetric aptasensor exhibited high sensitivity, specificity and stability and a $3.1 \text{ ng}\cdot\text{mL}^{-1}$ (80 $\mu\text{mol/L}$) thrombin detection limit.

A signal-on G4 electrochemical aptasensor based on co-immobilization of MP-11 and thiol ferrocene-labeled anti-thrombin aptamer, the interaction being detected via a microperoxidase-mediated electron transfer between the ferrocene and the gold electrode surface, was described [84]. The system showed a very high sensitivity of 30 fM using electrochemical impedance spectroscopy. Another impedimetric aptasensor for thrombin, based on a layer-by-layer polyamidoamine dendrimer-modified gold electrode [91], showed in the presence of the reversible $[\text{Fe}(\text{CN})_6]^{3-/4-}$ redox couple a linear relationship with the concentrations of thrombin in the range of 1–50 nM and a 0.01 nM detection limit.

More recently, a signal-on electrochemical aptasensor based on target-induced split aptamer fragments' conjunction was described [86]. The new design used TBA splinted into two fragments, one attached to the gold electrode and the second one modified with ferrocene, the association of thrombin inducing the association of the two fragments, thus increasing the concentration of ferrocene at the electrode surface. The signal-on electrochemical aptasensor showed a linear range of 0.8–15 nM and a 0.2 nM detection limit.

Another procedure used to improve the sensitivity of the G4 electrochemical aptasensors for the detection of thrombin used an amplification strategy based on the electrochemical active-inactive switch between monomer/dimer forms of carminic acid (CA). The CA was electroactive, while the CA dimers were electrochemically inactive [92]. With magnetic enrichment, the sensor showed a 42.4 pM detection limit.

Nanoparticle-based materials, including gold [63,73], platinum [57] and Fe_3O_4 nanoparticles [93] and quantum dot-coated silica nanospheres [94], were also used as signal amplification strategies for ultrasensitive electrochemical aptasensing. For example, an electrochemical aptasensor based on gold nanoparticles showed a linear range of 0.05–18 nM and a 0.02 nM detection limit [63], while another one based on Fe_3O_4 -nanoparticles [93] showed a linear response for thrombin in the range of 1.0–75 nM and a 0.1 nM detection limit.

Based on the aptamer conformational change in the presence of K^+ cations, different electrochemical aptasensors have been developed for selective potassium recognition. The formation of a G4 structure in the presence of K^+ ions was detected by monitoring the changes on the electron transfer between redox labels and the electrode surface [95–97] or by detecting the changes on the interfacial electron transfer resistance [98]. The same strategy for specific recognition of other metal ions, such as Tb^{3+} , was used [99].

Taking advantage of the ability of thrombin to catalyze the hydrolysis of the peptide (-Ala-Gly-Arg-nitroaniline) to nitroaniline, thrombin was electrochemically detected, by quantifying the nitroaniline reaction product [56].

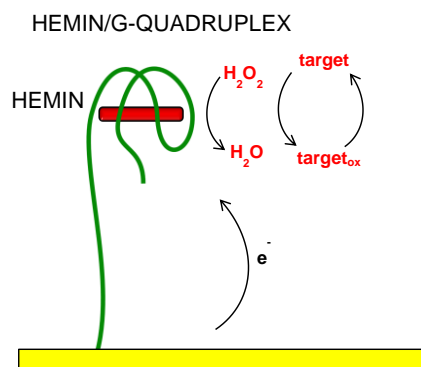
A different strategy for G4 electrochemical aptasensors used catalysts, such as horseradish peroxidase (HRP) [56,100]. In a simple approach, TBA was non-specifically immobilized on the electrode surface, and thrombin was detected using the HRP label, allowing a 3.5 nM detection limit, sufficient for clinical diagnostic of metastatic lung cancer, where the concentration of thrombin level detected was 5.4 nM [56].

An impedimetric biosensor based on a DNA aptamer specific to ochratoxin A (OTA) covalently immobilized onto a mixed Langmuir–Blodgett monolayer composed of polyaniline-stearic acid and deposited on indium tin oxide (ITO)-coated glass plates showed a 0.24 nM detection limit [85]. The system was further improved [87], showing a detection limit comparable to that of the HPLC method (0.12 nM), and was validated in food samples. Another design for the OTA detection proposed the use of a long polyethylene glycol spacer chain, which led to the formation of long tunnels at the surface of screen-printed carbon electrodes, with aptamers acting as gates. The aptamer changed configuration after OTA binding, and the peak current decreased [88].

In a different approach, OTA was detected at a G4 electrochemical aptasensor that used a hairpin anti-OTA aptamer and site-specific DNA cleavage of TaqI restriction endonuclease, as well as a streptavidin-HRP tag, being able to detect as low as 0.4 pg/mL OTA with ultrahigh selectivity [100].

3.2. Hemin/G4 DNAzyme Electrochemical Biosensor

Hemin/G4 DNAzyme is an artificial catalytically-active DNA molecule (DNAzyme) that is composed of DNA in the G4 configuration with intercalated hemin molecules. Hemin is an iron-containing porphyrin, whose peroxidase activity increases in the presence of DNA, facilitating the redox reaction between H_2O_2 and a target molecule (the substrate, e.g., 3,3',5,5'-tetramethylbenzidine, hydroquinone or ferrocene methyl alcohol), which results in the appearance of an oxidized target molecule (the electroactive product), that is electrochemically detected (Scheme 5).



Scheme 5. Hemin/G4 peroxidase-mimicking DNAzyme electrochemical biosensor. Adapted from [19] with permission.

Hemin/G4 DNAzyme electrochemical biosensors represent nowadays one of the most popular building assays of G4-based electrochemical biosensors [101]. The most common strategy consists of the modification of the electrode by a hairpin nucleic acid oligonucleotide that contains two sequences,

a sequence capable of forming a G4 structure that binds the hemin, used as the amplification strategy, and an aptamer able to specifically bind the analyte, which might form or not a G4 structure. In the presence of the analyte and hemin, the hairpin structures are opened, the hemin/G4 structures are formed on the electrode surface, while the analyte binds to the aptamer.

Since the first report on using hemin/G4 DNAzyme as the electrocatalytic label for amplifying sensing events [102], this approach attracted increasing interest in biosensor [103,104] and biofuel cell technologies [105]. In comparison with protein peroxidases, the hemin/G4 peroxidase-mimicking DNAzymes have several advantages, such as high chemical stability, low cost and simple synthesis. Hemin/G4 DNAzyme electrochemical biosensors were successfully used for the detection of cells [106,107], proteins [108–110] or low molecular weight molecules, such as adenosine monophosphate (AMP) [102,111,112], anticancer drugs [113], gaseous ligands [114], toxins [115,116], pollutant agents [117,118] or metal ions [119,120].

Later on, more complicated amplification strategies were developed to improve the sensitivity of the hemin/G4 DNAzyme HRP-mimicking activity, such as dual-amplification [121], background noise reduction [122] or autocatalytic target recycling strategies [123].

The glucose oxidase activity was followed by a hemin/G4 DNAzyme electrochemical biosensor, by attaching the enzyme to the electrode surface through the nucleic acid sequence able to form G4s in the presence of hemin [102,124]. Then, the glucose oxidase mediated the glucose oxidation to gluconic acid and H_2O_2 , and the resulting H_2O_2 was analyzed through its electrocatalyzed reduction by the DNAzyme.

Another electrochemical sensing strategy, based on the G4 DNAzyme for the detection of both adenosines and hydrogen peroxide from cancer cells, was developed [112], which detected the flux of H_2O_2 released from cells with high sensitivity and showed a 0.1 nM detection limit for ATP.

A hemin/G4 DNAzyme-based impedimetric biosensor was used to detect the environmental metabolite 2-hydroxyfluorene (2-HOFlu) [117], using the hemin/G4 HRP-like activity to catalyze the oxidation of 2-HOFlu by H_2O_2 , with a 1.2 nM detection limit in water and a 3.6 nM detection limit in spiked lake water samples. The assay was also selective over other fluorene derivatives.

A sandwich-type electrochemical aptamer cytosensor for the detection of HepG2 cells was used [106]. On the first approach, the sensor was built up by self-assembling thiolated TLS11a aptamers on the surface of gold electrodes and a G4/hemin/aptamer and HRP-modified gold nanoparticles. The sensor detection range was from 10^2 – 10^7 cells·mL⁻¹ and had a 30 cells·mL⁻¹ low detection limit.

The system was improved by self-assembling the TLS11a aptamers with gold nanoparticles (AuNPs) on the surface of GCE [107]. Hybrid Fe_3O_4 /MnO₂/Au@Pd nanoelectrocatalysts, hemin/G4 HRP-mimicking DNAzymes and the natural HRP enzyme efficiently amplified the electrochemical signal through catalyzing the oxidation of hydroquinone (HQ) by H_2O_2 . This cytosensor provided a better 15 cells·mL⁻¹ detection limit, good specificity and stability.

In a different approach, the hemin/G4 DNAzyme electrochemical biosensors took advantage of the hemin/G4 acting both as an NADH oxidase, assisting the oxidation of NADH to NAD⁺ together with the generation of H_2O_2 in the presence of dissolved O₂, as well as a hemin/G4 DNAzyme to bioelectrocatalyze the reduction of the produced H_2O_2 . Initially, this approach was used for the detection of thrombin [125–127]. More recently, the Pebrine disease-related *Nosema bombycis* spore wall protein was detected, using the amplification of hemin/G4 DNAzyme functionalized with Pt@Pd nanowires, the electrochemical immunosensor exhibiting a linear range from 0.001 – 100 ng·mL⁻¹ and a 0.24 pg·mL⁻¹ detection limit [128].

A DNAzyme that simultaneously served as an NADH oxidase and HRP-mimicking DNAzyme was developed to detect mercury ions (Hg²⁺) [129], with the dynamic concentration range spanning from 1.0 ng L⁻¹– 10 mg·L⁻¹ Hg²⁺ and a 0.5 ng·L⁻¹ (2.5 pM) detection limit, also demonstrating an excellent selectivity against other interferent metal ions.

A pseudo triple-enzyme cascade electrocatalytic electrochemical aptasensor for the determination of thrombin, using the amplification of an alcohol dehydrogenase (ADH)-Pt-Pd nanowire bionanocomposite and a hemin/G4 structure that simultaneously acted as NADH oxidase and

HRP-mimicking DNAzyme, was developed [130]. The ADH immobilized on the Pt-Pd nanowires catalyzed the ethanol present in the electrolyte into acetaldehyde, accompanied by NAD^+ being converted to NADH. Then, the hemin/G4 firstly served as NADH oxidase, converting the produced NADH to NAD^+ , then the hemin/G4 acting as the HRP-mimicking DNAzyme bioelectrocatalyzed the produced H_2O_2 . In this way, a concentration linear range from 0.2 pM–20 nM with a low 0.067 pM detection limit for thrombin was obtained.

Another strategy for thrombin detection consisted of using porous platinum nanotubes (PtNTs) labelled with hemin/G4 and GDH [131]. Coupling with GDH and hemin/G4 as NADH oxidase and HRP-mimicking DNAzyme, the cascade signal amplification allowed the detection limit of thrombin down to the 0.15 pM level.

4. Conclusions

The detailed knowledge of G4 formation mechanism, at the surface of electrochemical transducers, is of utmost importance for the design and fabrication of G4-based electrochemical aptasensors, with applications in nanotechnology and biosensor technology. The voltammetric techniques in combination with AFM were successfully employed to study the transformation of single-strand sequences into the G4 configuration or G4-based nanostructures, in freshly-prepared solutions, for concentrations 10-times lower than usually detected by other techniques, such as UV absorbance, circular dichroism or electrospay mass spectroscopy.

The key features of the G4 conformation in nucleic acid electrochemistry and their application in G4 electrochemical biosensors that use redox labels as amplification strategies, i.e., the G4 electrochemical aptasensors and the hemin/G4 HRP-mimicking DNAzyme electrochemical biosensors, were revised.

Acknowledgments: Financial support from Fundação para a Ciência e Tecnologia (FCT), Grants SFRH/BPD/92726/2013 (Ana-Maria Chiorcea-Paquim), projects PTDC/SAU-BMA/118531/2010, PTDC/QEQ-MED/0586/2012, UID/EMS/00285/2013 (co-financed by the European Community Fund FEDER), FEDER funds through the program COMPETE—Programa Operacional Factores de Competitividade is gratefully acknowledged.

Conflicts of Interest: the authors declare no conflict of interest.

References

1. Mergny, J.-L.; De Cian, A.; Ghelab, A.; Saccà, B.; Lacroix, L. Kinetics of Tetramolecular Quadruplexes. *Nucleic Acids Res.* **2005**, *33*, 81–94.
2. Neidle, S. *Therapeutic Applications of Quadruplex Nucleic Acids*; Elsevier: Amsterdam, The Netherlands, 2012.
3. Simonsson, T. G-quadruplex DNA structures-variations on a theme. *Biol. Chem.* **2001**, *382*, 621–628.
4. Tran, P.L.T.; De Cian, A.; Gros, J.; Moriyama, R.; Mergny, J.-L. Tetramolecular Quadruplex stability and assembly. *Top. Curr. Chem.* **2013**, *330*, 243–273.
5. Zhang, S.; Wu, Y.; Zhang, W. G-quadruplex structures and their interaction diversity with ligands. *ChemMedChem* **2014**, *9*, 899–911.
6. Keniry, M.A. Quadruplex Structures in nucleic acids. *Biopolymers* **2000–2001**, *56*, 123–146.
7. Chambers, V.S.; Marsico, G.; Boutell, J.M.; Di Antonio, M.; Smith, G.P.; Balasubramanian, S. High-Throughput sequencing of DNA G-quadruplex structures in the human genome. *Nat. Biotechnol.* **2015**, *33*, 877–881.
8. Murat, P.; Balasubramanian, S. Existence and consequences of G-quadruplex structures in DNA. *Curr. Opin. Genet. Dev.* **2014**, *25*, 22–29.
9. Henderson, A.; Wu, Y.; Huang, Y.C.; Chavez, E.A.; Platt, J.; Johnson, F.B.; Brosh, R.M.; Sen, D.; Lansdorp, P.M. Detection of G-quadruplex DNA in mammalian cells. *Nucleic Acids Res.* **2014**, *42*, 860–869. [[CrossRef](#)] [[PubMed](#)]
10. Dailey, M.M.; Hait, C.; Holt, P.A.; Maguire, J.M.; Meier, J.B.; Miller, M.C.; Petraccone, L.; Trent, J.O. Structure-Based drug design: From Nucleic acid to membrane protein targets. *Exp. Mol. Pathol.* **2009**, *86*, 141–150. [[CrossRef](#)] [[PubMed](#)]
11. Todd, A.K.; Johnston, M.; Neidle, S. Highly prevalent putative quadruplex sequence motifs in human DNA. *Nucleic Acids Res.* **2005**, *33*, 2901–2907. [[CrossRef](#)] [[PubMed](#)]

12. Huppert, J.L. Hunting G-quadruplexes. *Biochimie* **2008**, *90*, 1140–1148. [[CrossRef](#)] [[PubMed](#)]
13. Huppert, J.L.; Balasubramanian, S. Prevalence of quadruplexes in the human genome. *Nucleic Acids Res.* **2005**, *33*, 2908–2916. [[CrossRef](#)] [[PubMed](#)]
14. Chiorcea-Paquim, A.-M.; Oliveira-Brett, A.M. Redox behaviour of G-quadruplexes. *Electrochim. Acta* **2014**, *126*, 162–170. [[CrossRef](#)]
15. Artandi, S.E.; DePinho, R.A. *Telomeres and Telomerase in Cancer*; Hiyama, K., Ed.; Humana Press: Totowa, NJ, USA, 2009.
16. Neidle, S. The structures of quadruplex nucleic acids and their drug complexes. *Curr. Opin. Struct. Biol.* **2009**, *19*, 239–250. [[CrossRef](#)] [[PubMed](#)]
17. Borovok, N.; Iram, N.; Zikich, D.; Ghabboun, J.; Livshits, G.I.; Porath, D.; Kotlyar, A.B. Assembling of G-strands into novel tetra-molecular parallel g4-dna nanostructures using avidin-biotin recognition. *Nucleic Acids Res.* **2008**, *36*, 5050–5060. [[CrossRef](#)] [[PubMed](#)]
18. Borovok, N.; Molotsky, T.; Ghabboun, J.; Porath, D.; Kotlyar, A. Efficient procedure of preparation and properties of long uniform G4-dna nanowires. *Anal. Biochem.* **2008**, *374*, 71–78. [[CrossRef](#)] [[PubMed](#)]
19. Gray, R.D.; Trent, J.O.; Chaires, J.B. Folding and Unfolding pathways of the human telomeric G-quadruplex. *J. Mol. Biol.* **2014**, *426*, 1629–1650. [[CrossRef](#)] [[PubMed](#)]
20. Karsisiotis, A.I.; Webba da Silva, M. Structural probes in quadruplex nucleic acid structure determination by NMR. *Molecules* **2012**, *17*, 13073–13086. [[CrossRef](#)] [[PubMed](#)]
21. Adrian, M.; Heddi, B.; Phan, A.T. NMR spectroscopy of G-quadruplexes. *Methods* **2012**, *57*, 11–24. [[CrossRef](#)] [[PubMed](#)]
22. Sun, D.; Hurley, L.H. Biochemical Techniques for the characterization of G-quadruplex structures: EMSA, DMS footprinting, and DNA polymerase stop assay. *Methods Mol. Biol.* **2010**, *608*, 65–79. [[PubMed](#)]
23. Jaumot, J.; Gargallo, R. Experimental methods for studying the interactions between G-quadruplex structures and ligands. *Curr. Pharm. Des.* **2012**, *18*, 1900–1916. [[CrossRef](#)] [[PubMed](#)]
24. Oliveira Brett, A.M.; Serrano, S.H.P.; Piedade, A.J.P. *Applications of Kinetic Modelling*; Comprehensive Chemical Kinetics; Elsevier: Amsterdam, The Netherlands, 1999; Volume 37.
25. Oliveira Brett, A.M. *Biosensors and Modern Biospecific Analytical Techniques*; Comprehensive Analytical Chemistry; Elsevier: Amsterdam, The Netherlands, 2005; Volume 44.
26. Brett, A.M.O. Electrochemistry for probing DNA damage. In *Encyclopedia of Sensors*; Grimes, C.A., Dickey, E.C., Pishko, M.V., Eds.; American Scientific Publishers: Valencia, CA, USA, 2006; p. 301.
27. Oliveira-Brett, A.M.; Paquim, A.M.C.; Diculescu, V.C.; Piedade, J.A.P. Electrochemistry of nanoscale DNA surface films on carbon. *Med. Eng. Phys.* **2006**, *28*, 963–970. [[CrossRef](#)] [[PubMed](#)]
28. Oliveira Brett, A.M.; Diculescu, V.C.; Chiorcea-Paquim, A.M.; Serrano, S.H.P. *Electrochemical Sensor Analysis*; Comprehensive Analytical Chemistry; Elsevier: Amsterdam, The Netherlands, 2007; Volume 49.
29. Oliveira Brett, A.M. Electrochemical DNA assays. In *Bioelectrochemistry: Fundamentals, Experimental Techniques and Applications*; Bartlett, P.N., Ed.; John Wiley & Sons, Ltd.: Chichester, UK, 2008; p. 411.
30. Oliveira-Brett, A.-M. Nanobioelectrochemistry. In *Electrochemistry at the Nanoscale, Nanostructures Science and Technology*; Schmuki, P., Virtanen, S., Eds.; Nanostructure Science and Technology; Springer New York: New York, NY, USA, 2009; p. 407.
31. Diculescu, V.C.; Chiorcea-Paquim, A.-M.; Oliveira-Brett, A.M. Applications of a DNA-electrochemical biosensor. *TrAC Trends Anal. Chem.* **2016**, *79*, 23–36. [[CrossRef](#)]
32. Chiorcea-Paquim, A.-M.; Santos, P.; Diculescu, V.C.; Eritja, R.; Oliveira-Brett, A.M. Guanine Quartets. In *Guanine Quartets: Structure and Application*; Spindler, L., Fritzsche, W., Eds.; Royal Society of Chemistry: Cambridge, UK, 2012; pp. 100–109.
33. Hianik, T.; Wang, J. Electrochemical aptasensors—Recent achievements and perspectives. *Electroanalysis* **2009**, *21*, 1223–1235. [[CrossRef](#)]
34. Musumeci, D.; Montesarchio, D. Polyvalent nucleic acid aptamers and modulation of their activity: A focus on the thrombin binding aptamer. *Pharmacol. Ther.* **2012**, *136*, 202–215. [[CrossRef](#)] [[PubMed](#)]
35. Tucker, W.O.; Shum, K.T.; Tanner, J.A. G-quadruplex DNA aptamers and their ligands: Structure, function and application. *Curr. Pharm. Des.* **2012**, *18*, 2014–2026. [[CrossRef](#)] [[PubMed](#)]
36. Ni, X.; Castanares, M.; Mukherjee, A.; Lupold, S.E. Nucleic Acid Aptamers: Clinical Applications and Promising New Horizons. *Curr. Med. Chem.* **2011**, *18*, 4206–4214. [[CrossRef](#)] [[PubMed](#)]

37. Diculescu, V.C.; Chiorcea-Paquim, A.-M.; Eritja, R.; Oliveira-Brett, A.M. Thrombin-binding Aptamer quadruplex formation: Afm and voltammetric characterization. *J. Nucleic Acids* **2010**, *2010*, 841932. [[CrossRef](#)] [[PubMed](#)]
38. Diculescu, V.C.; Chiorcea-Paquim, A.-M.; Eritja, R.; Oliveira-Brett, A.M. Evaluation of the Structure–activity Relationship of Thrombin with Thrombin Binding Aptamers by Voltammetry and Atomic Force Microscopy. *J. Electroanal. Chem.* **2011**, *656*, 159–166. [[CrossRef](#)]
39. Chiorcea-Paquim, A.-M.; Santos, P.V.; Oliveira-Brett, A.M. Atomic force microscopy and voltammetric characterisation of synthetic homo-oligodeoxynucleotides. *Electrochim. Acta* **2013**, *110*, 599–607. [[CrossRef](#)]
40. Chiorcea-Paquim, A.-M.; Santos, P.V.; Eritja, R.; Oliveira-Brett, A.M. Self-Assembled G-Quadruplex Nanostructures: AFM and Voltammetric Characterization. *Phys. Chem. Chem. Phys.* **2013**, *15*, 9117–9124. [[CrossRef](#)] [[PubMed](#)]
41. Rodrigues Pontinha, A.D.; Chiorcea-Paquim, A.-M.; Eritja, R.; Oliveira-Brett, A.M. Quadruplex Nanostructures of d(TGGGGT): Influence of Sodium and Potassium Ions. *Anal. Chem.* **2014**, *86*, 5851–5857. [[CrossRef](#)] [[PubMed](#)]
42. Chiorcea-Paquim, A.-M.; Pontinha, A.D.R.; Oliveira-Brett, A.M. Time-Dependent Polyguanylic Acid Structural Modifications. *Electrochem. Commun.* **2014**, *45*, 71–74. [[CrossRef](#)]
43. Chiorcea-Paquim, A.-M.; Rodrigues Pontinha, A.D.; Oliveira-Brett, A.M. Quadruplex-Targeting Anticancer Drug BRACO-19 Voltammetric and AFM Characterization. *Electrochim. Acta* **2015**, *174*, 155–163. [[CrossRef](#)]
44. Pontinha, A.D.R.; Sparapani, S.; Neidle, S.; Oliveira-Brett, A.M. Triazole-Acridine Conjugates: Redox Mechanisms and in Situ Electrochemical Evaluation of Interaction with Double-Stranded DNA. *Bioelectrochemistry* **2013**, *89*, 50–56. [[CrossRef](#)] [[PubMed](#)]
45. Chiorcea-Paquim, A.-M.; Pontinha, A.D.R.; Eritja, R.; Lucarelli, G.; Sparapani, S.; Neidle, S.; Oliveira-Brett, A.M. Atomic Force Microscopy and Voltammetric Investigation of Quadruplex Formation between a Triazole-Acridine Conjugate and Guanine-Containing Repeat DNA Sequences. *Anal. Chem.* **2015**, *87*, 6141–6149. [[CrossRef](#)] [[PubMed](#)]
46. Oliveira Brett, A.M.; Diculescu, V.C.; Chiorcea Paquim, A.-M.; Serrano, S. Chapter 20 DNA-Electrochemical Biosensors for Investigating DNA Damage. *Compr. Anal. Chem.* **2007**, *49*, 413–437.
47. Diculescu, V.C.; Chiorcea Paquim, A.-M.; Oliveira Brett, A.M. Electrochemical DNA Sensors for Detection of DNA Damage. *Sensors* **2005**, *5*, 377–393. [[CrossRef](#)]
48. Vasilescu, A.; Marty, J.-L. Electrochemical Aptasensors for the Assessment of Food Quality and Safety. *TrAC Trends Anal. Chem.* **2016**, *79*, 60–70. [[CrossRef](#)]
49. Willner, I.; Zayats, M. Electronic Aptamer-Based Sensors. *Angew. Chem. Int. Ed.* **2007**, *46*, 6408–6418. [[CrossRef](#)] [[PubMed](#)]
50. Cheng, A.K.H.; Sen, D.; Yu, H.-Z. Design and Testing of Aptamer-Based Electrochemical Biosensors for Proteins and Small Molecules. *Bioelectrochemistry* **2009**, *77*, 1–12. [[CrossRef](#)] [[PubMed](#)]
51. Velasco-Garcia, M.; Missailidis, S. New Trends in Aptamer-Based Electrochemical Biosensors. *Gene Ther. Mol. Biol.* **2009**, *13*, 1–10.
52. Yin, X.-B. Functional Nucleic Acids for Electrochemical and Electrochemiluminescent Sensing Applications. *TrAC Trends Anal. Chem.* **2012**, *33*, 81–94. [[CrossRef](#)]
53. Hianik, T.; Ostatná, V.; Sonlajtnerova, M.; Grman, I. Influence of Ionic Strength, pH and Aptamer Configuration for Binding Affinity to Thrombin. *Bioelectrochemistry* **2007**, *70*, 127–133. [[CrossRef](#)] [[PubMed](#)]
54. Liu, J.; Cao, Z.; Lu, Y. Functional Nucleic Acid Sensors. *Chem. Rev.* **2009**, *109*, 1948–1998. [[CrossRef](#)] [[PubMed](#)]
55. Song, S.; Wang, L.; Li, J.; Fan, C.; Zhao, J. Aptamer-Based Biosensors. *TrAC Trends Anal. Chem.* **2008**, *27*, 108–117. [[CrossRef](#)]
56. Mir, M.; Vreeke, M.; Katakis, I. Different Strategies to Develop an Electrochemical Thrombin Aptasensor. *Electrochem. Commun.* **2006**, *8*, 505–511. [[CrossRef](#)]
57. Polsky, R.; Gill, R.; Kaganovsky, L.; Willner, I. Nucleic Acid-Functionalized Pt Nanoparticles: Catalytic Labels for the Amplified Electrochemical Detection of Biomolecules. *Anal. Chem.* **2006**, *78*, 2268–2271. [[CrossRef](#)] [[PubMed](#)]
58. Numnuam, A.; Chumbimuni-Torres, K.Y.; Xiang, Y.; Bash, R.; Thavarungkul, P.; Kanatharana, P.; Pretsch, E.; Wang, J.; Bakker, E. Aptamer-Based Potentiometric Measurements of Proteins Using Ion-Selective Microelectrodes. *Anal. Chem.* **2008**, *80*, 707–712. [[CrossRef](#)] [[PubMed](#)]

59. Yang, H.; Ji, J.; Liu, Y.; Kong, J.; Liu, B. An Aptamer-Based Biosensor for Sensitive Thrombin Detection. *Electrochem. Commun.* **2009**, *11*, 38–40. [[CrossRef](#)]
60. Peng, K.; Zhao, H.; Wu, X.; Yuan, Y.; Yuan, R. Ultrasensitive Aptasensor Based on Graphene-3,4,9,10-Perylenetetra-carboxylic Dianhydride as Platform and Functionalized Hollow PtCo Nanochains as Enhancers. *Sens. Actuators B Chem.* **2012**, *169*, 88–95. [[CrossRef](#)]
61. Centi, S.; Messina, G.; Tombelli, S.; Palchetti, I.; Mascini, M. Different Approaches for the Detection of Thrombin by an Electrochemical Aptamer-Based Assay Coupled to Magnetic Beads. *Biosens. Bioelectron.* **2008**, *23*, 1602–1609. [[CrossRef](#)] [[PubMed](#)]
62. Centi, S.; Tombelli, S.; Minunni, M.; Mascini, M. Aptamer-Based Detection of Plasma Proteins by an Electrochemical Assay Coupled to Magnetic Beads. *Anal. Chem.* **2007**, *79*, 1466–1473. [[CrossRef](#)] [[PubMed](#)]
63. Li, B.; Wang, Y.; Wei, H.; Dong, S. Amplified Electrochemical Aptasensor Taking AuNPs Based Sandwich Sensing Platform as a Model. *Biosens. Bioelectron.* **2008**, *23*, 965–970. [[CrossRef](#)] [[PubMed](#)]
64. Ikebukuro, K.; Kiyohara, C.; Sode, K. Electrochemical Detection of Protein Using a Double Aptamer Sandwich. *Anal. Lett.* **2004**, *37*, 2901–2909. [[CrossRef](#)]
65. Ikebukuro, K.; Kiyohara, C.; Sode, K. Novel Electrochemical Sensor System for Protein Using the Aptamers in Sandwich Manner. *Biosens. Bioelectron.* **2005**, *20*, 2168–2172. [[CrossRef](#)] [[PubMed](#)]
66. Kang, Y.; Feng, K.-J.; Chen, J.-W.; Jiang, J.-H.; Shen, G.-L.; Yu, R.-Q. Electrochemical Detection of Thrombin by Sandwich Approach Using Antibody and Aptamer. *Bioelectrochemistry* **2008**, *73*, 76–81. [[CrossRef](#)] [[PubMed](#)]
67. Rahman, M.A.; Son, J.I.; Won, M.-S.; Shim, Y.-B. Gold Nanoparticles Doped Conducting Polymer Nanorod Electrodes: Ferrocene Catalyzed Aptamer-Based Thrombin Immunosensor. *Anal. Chem.* **2009**, *81*, 6604–6611. [[CrossRef](#)] [[PubMed](#)]
68. Lubin, A.A.; Plaxco, K.W. Folding-Based Electrochemical Biosensors: The Case for Responsive Nucleic Acid Architectures. *Acc. Chem. Res.* **2010**, *43*, 496–505. [[CrossRef](#)] [[PubMed](#)]
69. Plaxco, K.W.; Soh, H.T. Switch-Based Biosensors: A New Approach towards Real-Time, in Vivo Molecular Detection. *Trends Biotechnol.* **2011**, *29*, 1–5. [[CrossRef](#)] [[PubMed](#)]
70. Bai, H.-Y.; Del Campo, F.J.; Tsai, Y.-C. Sensitive Electrochemical Thrombin Aptasensor Based on Gold Disk Microelectrode arrays. *Biosens. Bioelectron.* **2013**, *42*, 17–22. [[CrossRef](#)] [[PubMed](#)]
71. Xu, H.; Gorgy, K.; Gondran, C.; Le Goff, A.; Spinelli, N.; Lopez, C.; Defrancq, E.; Cosnier, S. Label-Free Impedimetric Thrombin Sensor Based on Poly(pyrrole-Nitrilotriacetic Acid)-Aptamer Film. *Biosens. Bioelectron.* **2013**, *41*, 90–95. [[CrossRef](#)] [[PubMed](#)]
72. Li, X.; Shen, L.; Zhang, D.; Qi, H.; Gao, Q.; Ma, F.; Zhang, C. Electrochemical Impedance Spectroscopy for Study of Aptamer-Thrombin Interfacial Interactions. *Biosens. Bioelectron.* **2008**, *23*, 1624–1630. [[CrossRef](#)] [[PubMed](#)]
73. Suprun, E.; Shumyantseva, V.; Bulko, T.; Rachmetova, S.; Rad'ko, S.; Bodoev, N.; Archakov, A. Au-Nanoparticles as an Electrochemical Sensing Platform for Aptamer-Thrombin Interaction. *Biosens. Bioelectron.* **2008**, *24*, 831–836. [[CrossRef](#)] [[PubMed](#)]
74. Feng, L.; Chen, Y.; Ren, J.; Qu, X. A Graphene Functionalized Electrochemical Aptasensor for Selective Label-Free Detection of Cancer Cells. *Biomaterials* **2011**, *32*, 2930–2937. [[CrossRef](#)] [[PubMed](#)]
75. Elahi, M.Y.; Bathaie, S.Z.; Mousavi, M.F.; Hoshyar, R.; Ghasemi, S. A New DNA-Nanobiosensor Based on G-Quadruplex Immobilized on Carbon Nanotubes Modified Glassy Carbon Electrode. *Electrochim. Acta* **2012**, *82*, 143–151. [[CrossRef](#)]
76. Xiao, Y.; Lubin, A.A.; Heeger, A.J.; Plaxco, K.W. Label-Free Electronic Detection of Thrombin in Blood Serum by Using an Aptamer-Based Sensor. *Angew. Chem.* **2005**, *117*, 5592–5595. [[CrossRef](#)]
77. Radi, A.-E.; Acero Sánchez, J.L.; Baldrich, E.; O'Sullivan, C.K. Reusable Impedimetric Aptasensor. *Anal. Chem.* **2005**, *77*, 6320–6323. [[CrossRef](#)] [[PubMed](#)]
78. Radi, A.-E.; Acero Sánchez, J.L.; Baldrich, E.; O'Sullivan, C.K. Reagentless, Reusable, Ultrasensitive Electrochemical Molecular Beacon Aptasensor. *J. Am. Chem. Soc.* **2006**, *128*, 117–124. [[CrossRef](#)] [[PubMed](#)]
79. Sánchez, J.L.A.; Baldrich, E.; Radi, A.E.-G.; Dondapati, S.; Sánchez, P.L.; Katakis, I.; O'Sullivan, C.K. Electronic “Off-On” Molecular Switch for Rapid Detection of Thrombin. *Electroanalysis* **2006**, *18*, 1957–1962. [[CrossRef](#)]
80. Bang, G.S.; Cho, S.; Kim, B.-G. A Novel Electrochemical Detection Method for Aptamer Biosensors. *Biosens. Bioelectron.* **2005**, *21*, 863–870. [[CrossRef](#)] [[PubMed](#)]
81. Yan, F.; Wang, F.; Chen, Z. Aptamer-Based Electrochemical Biosensor for Label-Free Voltammetric Detection of Thrombin and Adenosine. *Sens. Actuators B Chem.* **2011**, *160*, 1380–1385. [[CrossRef](#)]

82. Xiao, Y.; Piorek, B.D.; Plaxco, K.W.; Heeger, A.J. A Reagentless Signal-on Architecture for Electronic, Aptamer-Based Sensors via Target-Induced Strand Displacement. *J. Am. Chem. Soc.* **2005**, *127*, 17990–17991. [[CrossRef](#)] [[PubMed](#)]
83. Meini, N.; Farre, C.; Chaix, C.; Kherrat, R.; Dzyadevych, S.; Jaffrezic-Renault, N. A Sensitive and Selective Thrombin Impedimetric Aptasensor Based on Tailored Aptamers Obtained by Solid-Phase Synthesis. *Sens. Actuators B Chem.* **2012**, *166–167*, 715–720. [[CrossRef](#)]
84. Mir, M.; Jenkins, A.T.A.; Katakis, I. Ultrasensitive Detection Based on an Aptamer Beacon Electron Transfer Chain. *Electrochem. Commun.* **2008**, *10*, 1533–1536. [[CrossRef](#)]
85. Prabhakar, N.; Matharu, Z.; Malhotra, B.D. Polyaniline Langmuir-Blodgett Film Based Aptasensor for Ochratoxin A Detection. *Biosens. Bioelectron.* **2011**, *26*, 4006–4011. [[CrossRef](#)] [[PubMed](#)]
86. Chen, J.; Zhang, J.; Li, J.; Yang, H.-H.; Fu, F.; Chen, G. An Ultrasensitive Signal-on Electrochemical Aptasensor via Target-Induced Conjunction of Split Aptamer Fragments. *Biosens. Bioelectron.* **2010**, *25*, 996–1000. [[CrossRef](#)] [[PubMed](#)]
87. Castillo, G.; Lamberti, I.; Mosiello, L.; Hianik, T. Impedimetric DNA Aptasensor for Sensitive Detection of Ochratoxin A in Food. *Electroanalysis* **2012**, *24*, 512–520. [[CrossRef](#)]
88. Hayat, A.; Andreescu, S.; Marty, J.-L. Design of PEG-Aptamer Two Piece Macromolecules as Convenient and Integrated Sensing Platform: Application to the Label Free Detection of Small Size Molecules. *Biosens. Bioelectron.* **2013**, *45*, 168–173. [[CrossRef](#)] [[PubMed](#)]
89. Jalit, Y.; Gutierrez, F.A.; Dubacheva, G.; Goyer, C.; Coche-Guerente, L.; Defrancq, E.; Labbé, P.; Rivas, G.A.; Rodríguez, M.C. Characterization of a Modified Gold Platform for the Development of a Label-Free Anti-Thrombin Aptasensor. *Biosens. Bioelectron.* **2013**, *41*, 424–429. [[CrossRef](#)] [[PubMed](#)]
90. De Rache, A.; Kejnovská, I.; Vorlíčková, M.; Buess-Herman, C. Elongated Thrombin Binding Aptamer: A G-Quadruplex Cation-Sensitive Conformational Switch. *Chemistry* **2012**, *18*, 4392–4400. [[CrossRef](#)] [[PubMed](#)]
91. Zhang, Z.; Yang, W.; Wang, J.; Yang, C.; Yang, F.; Yang, X. A Sensitive Impedimetric Thrombin Aptasensor Based on Polyamidoamine Dendrimer. *Talanta* **2009**, *78*, 1240–1245. [[CrossRef](#)] [[PubMed](#)]
92. Cheng, G.; Shen, B.; Zhang, F.; Wu, J.; Xu, Y.; He, P.; Fang, Y. A New Electrochemically Active-Inactive Switching Aptamer Molecular Beacon to Detect Thrombin Directly in Solution. *Biosens. Bioelectron.* **2010**, *25*, 2265–2269. [[CrossRef](#)] [[PubMed](#)]
93. Zhang, S.; Zhou, G.; Xu, X.; Cao, L.; Liang, G.; Chen, H.; Liu, B.; Kong, J. Development of an Electrochemical Aptamer-Based Sensor with a Sensitive Fe₃O₄ Nanoparticle-Redox Tag for Reagentless Protein Detection. *Electrochem. Commun.* **2011**, *13*, 928–931. [[CrossRef](#)]
94. Li, Y.; Deng, L.; Deng, C.; Nie, Z.; Yang, M.; Si, S. Simple and Sensitive Aptasensor Based on Quantum Dot-Coated Silica Nanospheres and the Gold Screen-Printed Electrode. *Talanta* **2012**, *99*, 637–642. [[CrossRef](#)] [[PubMed](#)]
95. Radi, A.-E.; O'Sullivan, C.K. Aptamer Conformational Switch as Sensitive Electrochemical Biosensor for Potassium Ion Recognition. *Chem. Commun. (Camb.)* **2006**, *32*, 3432–3434. [[CrossRef](#)] [[PubMed](#)]
96. Wu, Z.-S.; Chen, C.-R.; Shen, G.-L.; Yu, R.-Q. Reversible Electronic Nanoswitch Based on DNA G-Quadruplex Conformation: A Platform for Single-Step, Reagentless Potassium Detection. *Biomaterials* **2008**, *29*, 2689–2696. [[CrossRef](#)] [[PubMed](#)]
97. Zhang, J.; Wan, Y.; Wang, L.; Song, S.; Li, D.; Fan, C. Switchable Charge Transport Path via a Potassium Ions Promoted Conformational Change of G-Quadruplex Probe Monolayer. *Electrochem. Commun.* **2008**, *10*, 1258–1260. [[CrossRef](#)]
98. Chen, Z.; Chen, L.; Ma, H.; Zhou, T.; Li, X. Aptamer Biosensor for Label-Free Impedance Spectroscopy Detection of Potassium Ion Based on DNA G-Quadruplex Conformation. *Biosens. Bioelectron.* **2013**, *48*, 108–112. [[CrossRef](#)] [[PubMed](#)]
99. Zhang, J.; Chen, J.; Chen, R.; Chen, G.; Fu, F. An Electrochemical Biosensor for Ultratrace Terbium Based on Tb³⁺ Promoted Conformational Change of Human Telomeric G-Quadruplex. *Biosens. Bioelectron.* **2009**, *25*, 378–382. [[CrossRef](#)] [[PubMed](#)]
100. Zhang, J.; Chen, J.; Zhang, X.; Zeng, Z.; Chen, M.; Wang, S. An Electrochemical Biosensor Based on Hairpin-DNA Aptamer Probe and Restriction Endonuclease for Ochratoxin A Detection. *Electrochem. Commun.* **2012**, *25*, 5–7. [[CrossRef](#)]

101. Han, G.; Feng, X.; Chen, Z. Hemin/G-Quadruplex DNAzyme for Designing of Electrochemical Sensors. *Int. J. Electrochem. Sci* **2015**.
102. Pelossof, G.; Tel-Vered, R.; Elbaz, J.; Willner, I. Amplified Biosensing Using the Horseradish Peroxidase-Mimicking DNAzyme as an Electrocatalyst. *Anal. Chem.* **2010**, *82*, 4396–4402. [[CrossRef](#)] [[PubMed](#)]
103. Kosman, J.; Juskowiak, B. Peroxidase-Mimicking DNAzymes for Biosensing Applications: A Review. *Anal. Chim. Acta* **2011**, *707*, 7–17. [[CrossRef](#)] [[PubMed](#)]
104. Kaneko, N.; Horii, K.; Kato, S.; Akitomi, J.; Waga, I. High-Throughput Quantitative Screening of Peroxidase-Mimicking DNAzymes on a Microarray by Using Electrochemical Detection. *Anal. Chem.* **2013**, *85*, 5430–5435. [[CrossRef](#)] [[PubMed](#)]
105. Zhang, M.; Xu, S.; Minteer, S.D.; Baum, D.A. Investigation of a Deoxyribozyme as a Biofuel Cell Catalyst. *J. Am. Chem. Soc.* **2011**, *133*, 15890–15893. [[CrossRef](#)] [[PubMed](#)]
106. Sun, D.; Lu, J.; Chen, Z.; Yu, Y.; Mo, M. A Repeatable Assembling and Disassembling Electrochemical Aptamer Cytosensor for Ultrasensitive and Highly Selective Detection of Human Liver Cancer Cells. *Anal. Chim. Acta* **2015**, *885*, 166–173. [[CrossRef](#)] [[PubMed](#)]
107. Sun, D.; Lu, J.; Zhong, Y.; Yu, Y.; Wang, Y.; Zhang, B.; Chen, Z. Sensitive Electrochemical Aptamer Cytosensor for Highly Specific Detection of Cancer Cells Based on the Hybrid Nanoelectrocatalysts and Enzyme for Signal Amplification. *Biosens. Bioelectron.* **2016**, *75*, 301–307. [[CrossRef](#)] [[PubMed](#)]
108. Li, D.; Shlyahovsky, B.; Elbaz, J.; Willner, I. Amplified Analysis of Low-Molecular-Weight Substrates or Proteins by the Self-Assembly of DNAzyme-Aptamer Conjugates. *J. Am. Chem. Soc.* **2007**, *129*, 5804–5805. [[CrossRef](#)] [[PubMed](#)]
109. Zhang, K.; Zhu, X.; Wang, J.; Xu, L.; Li, G. Strategy to Fabricate an Electrochemical Aptasensor: Application to the Assay of Adenosine Deaminase Activity. *Anal. Chem.* **2010**, *82*, 3207–3211. [[CrossRef](#)] [[PubMed](#)]
110. Yang, N.; Cao, Y.; Han, P.; Zhu, X.; Sun, L.; Li, G. Tools for Investigation of the RNA Endonuclease Activity of Mammalian Argonaute2 Protein. *Anal. Chem.* **2012**, *84*, 2492–2497. [[CrossRef](#)] [[PubMed](#)]
111. Liu, L.; Liang, Z.; Li, Y. Label Free, Highly Sensitive and Selective Recognition of Small Molecule Using Gold Surface Confined Aptamers. *Solid State Sci.* **2012**, *14*, 1060–1063. [[CrossRef](#)]
112. Wang, Z.-H.; Lu, C.-Y.; Liu, J.; Xu, J.-J.; Chen, H.-Y. An Improved G-Quadruplex DNAzyme for Dual-Functional Electrochemical Biosensing of Adenosines and Hydrogen Peroxide from Cancer Cells. *Chem. Commun. (Camb.)* **2014**, *50*, 1178–1180. [[CrossRef](#)] [[PubMed](#)]
113. Yang, Q.; Nie, Y.; Zhu, X.; Liu, X.; Li, G. Study on the Electrocatalytic Activity of Human Telomere G-Quadruplex-hemin Complex and Its Interaction with Small Molecular Ligands. *Electrochim. Acta* **2009**, *55*, 276–280. [[CrossRef](#)]
114. Zhu, X.; Zhang, W.; Xiao, H.; Huang, J.; Li, G. Electrochemical Study of a hemin-DNA Complex and Its Activity as a Ligand Binder. *Electrochim. Acta* **2008**, *53*, 4407–4413. [[CrossRef](#)]
115. Yang, C.; Lates, V.; Prieto-Simón, B.; Marty, J.-L.; Yang, X. Aptamer-DNAzyme Hairpins for Biosensing of Ochratoxin A. *Biosens. Bioelectron.* **2012**, *32*, 208–212. [[CrossRef](#)] [[PubMed](#)]
116. Zhu, Y.; Xu, L.; Ma, W.; Chen, W.; Yan, W.; Kuang, H.; Wang, L.; Xu, C. G-Quadruplex DNAzyme-Based Microcystin-LR (Toxin) Determination by a Novel Immunosensor. *Biosens. Bioelectron.* **2011**, *26*, 4393–4398. [[CrossRef](#)] [[PubMed](#)]
117. Liang, G.; Liu, X. G-Quadruplex Based Impedimetric 2-Hydroxyfluorene Biosensor Using Hemin as a Peroxidase Enzyme Mimic. *Microchim. Acta* **2015**, *182*, 2233–2240. [[CrossRef](#)]
118. Liang, G.; Liu, X.; Li, X. Highly Sensitive Detection of α -Naphthol Based on G-DNA Modified Gold Electrode by Electrochemical Impedance Spectroscopy. *Biosens. Bioelectron.* **2013**, *45*, 46–51. [[CrossRef](#)] [[PubMed](#)]
119. Zhang, Z.; Yin, J.; Wu, Z.; Yu, R. Electrocatalytic Assay of mercury(II) Ions Using a Bifunctional Oligonucleotide Signal Probe. *Anal. Chim. Acta* **2013**, *762*, 47–53. [[CrossRef](#)] [[PubMed](#)]
120. Pelossof, G.; Tel-Vered, R.; Willner, I. Amplified Surface Plasmon Resonance and Electrochemical Detection of Pb^{2+} Ions Using the Pb^{2+} -Dependent DNAzyme and hemin/G-Quadruplex as a Label. *Anal. Chem.* **2012**, *84*, 3703–3709. [[CrossRef](#)] [[PubMed](#)]
121. Yuan, Y.; Gou, X.; Yuan, R.; Chai, Y.; Zhuo, Y.; Mao, L.; Gan, X. Electrochemical Aptasensor Based on the Dual-Amplification of G-Quadruplex Horseradish Peroxidase-Mimicking DNAzyme and Blocking Reagent-Horseradish Peroxidase. *Biosens. Bioelectron.* **2011**, *26*, 4236–4240. [[CrossRef](#)] [[PubMed](#)]

122. Jiang, B.; Wang, M.; Li, C.; Xie, J. Label-Free and Amplified Aptasensor for Thrombin Detection Based on Background Reduction and Direct Electron Transfer of Hemin. *Biosens. Bioelectron.* **2013**, *43*, 289–292. [[CrossRef](#)] [[PubMed](#)]
123. Liu, S.; Wang, C.; Zhang, C.; Wang, Y.; Tang, B. Label-Free and Ultrasensitive Electrochemical Detection of Nucleic Acids Based on Autocatalytic and Exonuclease III-Assisted Target Recycling Strategy. *Anal. Chem.* **2013**, *85*, 2282–2288. [[CrossRef](#)] [[PubMed](#)]
124. Bai, L.; Yuan, R.; Chai, Y.; Yuan, Y.; Zhuo, Y.; Mao, L. Bi-Enzyme Functionized Hollow PtCo Nanochains as Labels for an Electrochemical Aptasensor. *Biosens. Bioelectron.* **2011**, *26*, 4331–4336. [[CrossRef](#)] [[PubMed](#)]
125. Xie, S.; Chai, Y.; Yuan, R.; Bai, L.; Yuan, Y.; Wang, Y. A Dual-Amplification Aptasensor for Highly Sensitive Detection of Thrombin Based on the Functionalized Graphene-Pd Nanoparticles Composites and the hemin/G-Quadruplex. *Anal. Chim. Acta* **2012**, *755*, 46–53. [[CrossRef](#)] [[PubMed](#)]
126. Yuan, Y.; Yuan, R.; Chai, Y.; Zhuo, Y.; Ye, X.; Gan, X.; Bai, L. Hemin/G-Quadruplex Simultaneously Acts as NADH Oxidase and HRP-Mimicking DNAzyme for Simple, Sensitive Pseudobienzyme Electrochemical Detection of Thrombin. *Chem. Commun. (Camb.)* **2012**, *48*, 4621–4623. [[CrossRef](#)] [[PubMed](#)]
127. Yuan, Y.; Liu, G.; Yuan, R.; Chai, Y.; Gan, X.; Bai, L. Dendrimer Functionalized Reduced Graphene Oxide as Nanocarrier for Sensitive Pseudobienzyme Electrochemical Aptasensor. *Biosens. Bioelectron.* **2013**, *42*, 474–480. [[CrossRef](#)] [[PubMed](#)]
128. Wang, Q.; Song, Y.; Chai, Y.; Pan, G.; Li, T.; Yuan, Y.; Yuan, R. Electrochemical Immunosensor for Detecting the Spore Wall Protein of *Nosema Bombycis* Based on the Amplification of hemin/G-Quadruplex DNAzyme Concatamers Functionalized Pt@Pd Nanowires. *Biosens. Bioelectron.* **2014**, *60*, 118–123. [[CrossRef](#)] [[PubMed](#)]
129. Yuan, Y.; Gao, M.; Liu, G.; Chai, Y.; Wei, S.; Yuan, R. Sensitive Pseudobienzyme Electrocatalytic DNA Biosensor for mercury(II) Ion by Using the Autonomously Assembled hemin/G-Quadruplex DNAzyme Nanowires for Signal Amplification. *Anal. Chim. Acta* **2014**, *811*, 23–28. [[CrossRef](#)] [[PubMed](#)]
130. Zheng, Y.; Chai, Y.; Yuan, Y.; Yuan, R. A Pseudo Triple-Enzyme Electrochemical Aptasensor Based on the Amplification of Pt-Pd Nanowires and hemin/G-Quadruplex. *Anal. Chim. Acta* **2014**, *834*, 45–50. [[CrossRef](#)] [[PubMed](#)]
131. Sun, A.; Qi, Q.; Wang, X.; Bie, P. Porous Platinum Nanotubes Labeled with hemin/G-Quadruplex Based Electrochemical Aptasensor for Sensitive Thrombin Analysis via the Cascade Signal Amplification. *Biosens. Bioelectron.* **2014**, *57*, 16–21. [[CrossRef](#)] [[PubMed](#)]



© 2016 by the authors; licensee MDPI, Basel, Switzerland. This article is an open access article distributed under the terms and conditions of the Creative Commons Attribution (CC-BY) license (<http://creativecommons.org/licenses/by/4.0/>).